PRAMANA — journal of physics

Vol. 81, No. 1
July 2013
pp. 87–101

A benchmark study on uncertainty of ALICE ASH 1.0, TALYS 1.0 and MCNPX 2.6 codes to estimate production yield of accelerator-based radioisotopes

SEYED AMIRHOSSEIN FEGHHI[1], ZOHREH GHOLAMZADEH*[,2], ZAHRA ALIPOOR[3], AKRAM ZALI[4], MAHDI JOHARIFARD[5], MORTEZA AREF[3] and CLAUDIO TENREIRO[2,6]

[1]Department of Radiation Application, Shahid Beheshti University, G.C., Tehran, Iran
[2]Department of Physics, Talca University, Talca, Chile
[3]Department of Physics, Zanjan University, Zanjan, Iran
[4]Department of Physics, Amirkabir University, Tehran, Iran
[5]Department of Physics, Firoozkooh Branch, Islamic Azad University, Firoozkooh, Iran
[6]Department of Energy Science, Sungkyunkwan University, 300 Cheoncheon-dong, Suwon, Korea
*Corresponding author. E-mail: cadmium_109@yahoo.com

MS received 8 December 2012; revised 11 March 2013; accepted 26 March 2013

Abstract. Radioisotopes find very important applications in various sectors of economic significance and their production is an important activity of many national programmes. Some deterministic codes such as ALICE ASH 1.0 and TALYS 1.0 are extensively used to calculate the yield of a radioisotope via numerical integral over the calculated cross-sections. MCNPX 2.6 stochastic code is more interesting among the other Monte Carlo-based computational codes for accessibility of different intranuclear cascade physical models to calculate the yield using experiment-based cross-sections. A benchmark study has been proposed to determine the codes' uncertainty in such calculations. ^{109}Cd, ^{86}Y and ^{85}Sr production yields by proton irradiation of silver, rubidium chloride and strontium carbonate targets are studied. ^{109}Cd, ^{86}Y and ^{85}Sr cross-sections are calculated using ALICE ASH 1.0 and TALYS 1.0 codes. The evaluated yields are compared with the experimental yields. The targets are modelled using MCNPX 2.6 code. The production yields are calculated using the available physical models of the code. The study shows acceptable relative discrepancies between theoretical and experimental results. Minimum relative discrepancy between experimental and theoretical yields is achievable using ISABEL intranuclear model in most of the targets simulated by MCNPX 2.6. The stochastic code utilization can be suggested for calculating ^{109}Cd, ^{86}Y and ^{85}Sr production yields. It results in more valid data than TALYS 1.0 and ALICE ASH 1.0 in noticeably less average relative discrepancies.

Keywords. Accelerator-based radioisotope; production yield; ALICE ASH 1.0; TALYS 1.0; MCNPX 2.6.

PACS Nos 24; 24.10.−i

DOI: 10.1007/s12043-013-0554-z; ***e*Publication: 28 June 2013**

1. Introduction

For preparing some benchmark documents for the routine production of a radioisotope, some experiments can be done using an accelerator while precise computation experiments provide more economical pathways in shorter times to estimate the yield from a suitable T(particle, x)R nuclear reaction. Moreover, computation methods can evaluate new designs without depending on trial experiments.

Some deterministic codes such as ALICE ASH 1.0 and TALYS 1.0 calculate reaction cross-sections using theoretical equations [1,2]. MCNPX 2.6 utilizes experiment-based cross-section libraries and can stochastically compute an irradiation process to generate a readable output file for HTAPE3X execute file and IOPT card [3,4].

Hence, a benchmark study on ALICE ASH 1.0 and TALYS 1.0 deterministic codes and MCNPX 2.6 stochastic code's ability to estimate production yield of radioisotopes as precisely as possible has been proposed in the present study.

1.1 *ALICE ASH 1.0*

The ALICE ASH code is a modified and advanced version of the ALICE code. The geometry-dependent hybrid (GDH) model is used for describing the pre-equilibrium particle emission. Intranuclear transition rates are calculated using the effective cross-section of nucleon–nucleon interactions in nuclear matter. Corrections are made to the GDH model for treating the effects in peripheral nuclear regions. The number of neutrons and protons for initial exciton state is calculated using realistic nucleon–nucleon interaction cross-sections in the nucleus. The exciton coalescence model and the knock-out model are used for describing the pre-equilibrium complex particle emission. The equilibrium emission of particles is described by the Weisskopf–Ewing model without detailed consideration of angular momentum.

The code calculates multiple particle emission, evaporation including fission competition, pre-compound decay, single and double differential spectra and cross-sections of the reaction products [1].

1.2 *TALYS 1.0*

TALYS is a software that simulates nuclear reactions which involve neutrons, γ-rays, protons, deuterons, tritons, helions and α-particles, in the 1 keV–200 MeV energy range. A group of nuclear reaction models has been implemented into a single code system, enabling a user to evaluate basically all nuclear reactions beyond the resonance range. For energies above a few MeV, pre-equilibrium reactions play an important role. For nucleon reactions, a two-component exciton model with a new form for the internal transition rates, which yields an improved description of pre-equilibrium processes over the whole energy range have been implemented in the code. Compound nucleus reactions are calculated using the Hauser–Feshbach formalism. For the first, binary interaction of the projectile and the nucleus, width fluctuation corrections (WFC) are included to account for the correlations that exist between the incident and outgoing waves [2].

1.3 *Particle's stopping power calculation using SRIM code*

SRIM 2006 is included in complete plots showing the experimental/theoretical, stopping of any ion in any elemental target, contained over 22,000 experimental data points reported since 1899.

The required thickness of the target can be calculated using the stopping and range of ions in matter (SRIM) code which is a group of programs which calculates the stop and range of ions (up to 2 GeV/amu) into matter using quantum mechanical treatment of ion–atom collisions. This calculation is made very efficient using statistical algorithms which allow the ions to jump between calculated collisions. Then the code calculates the average of the collision results over the intervening gap.

The physical thickness of the target layer is chosen, for a given beam/target angle geometry, to provide light–particle exit energy. It is advisable to minimize the thickness of the target layer to perform irradiations on 6° target geometry. In cyclotron production of radionuclides, the reaction cross-section data play a very important role. One needs full excitation function of the nuclear process to be able to calculate and predict the yield with reasonable accuracy. From a given excitation function, the expected yield of a product for a certain energy range, related to the target thickness, can be calculated using the expression [5]

$$\text{Yield} = \frac{N_A I H(1 - e^{-\lambda t})}{M} \int \frac{\sigma(E)}{S_p(E)} dE \quad \text{(MBq)}, \tag{1}$$

where N_A is the Avogadro number, I is the number of particles (#/S), H is the isotope abundance, λ is the decay constant, M is the target mass number, $\sigma(E)$ is the cross-section (mb), $S_p(E)$ is the target stopping power (MeV·cm^2/mg).

1.4 *MCNPX 2.6 code*

MCNPX^{TM} is a general purpose Monte Carlo radiation transport code designed to track particle types over broad ranges of energies. It is the next generation code in the series of Monte Carlo transport codes that began at Los Alamos National Laboratory nearly 60 years ago. MCNPX 2.6 is the latest code released by Radiation Safety Information Computational Center (RSICC) after the 2005 release of MCNPX 2.5.

MCNPX 2.6 has many new capabilities, particularly in the areas of transmutation, burn-up and delayed particle production. Many new tally sources and variance-reduction options have been developed. Physics improvements include a new version of the cascade-exciton model (CEM), the addition of the Los Alamos quark-gluon string model (LAQGSM) option, and a substantial upgrade to muon physics.

The code involves extension of neutron, proton and photonuclear libraries to 150 MeV; and the formulation of new variance-reduction and data analysis techniques. The program also includes cross-section measurements, benchmark experiments, deterministic code development and improvements in transmutation code and library tools through the CINDER90 project.

The code is designed to track 34 particle types over broad ranges of energies. The code covers many applications such as

- Design of accelerator spallation targets, particularly for neutron scattering facilities.

- Investigations for accelerator isotope production and destruction programs including the transmutation of nuclear waste.
- Research into accelerator-driven energy sources.
- Accelerator-based imaging technology such as neutron and proton radiography.
- Design of shielding in accelerator facilities.
- Transmutation, activation and burn-up in reactor and other systems.
- Nuclear criticality safety.
- Medical fields and so on.

The MCNPX code allows the user to choose between different intranuclear cascade and fission evaporation model combinations among ISABEL, BERTINI and INCL4 for cascade and DRESNER (associated with RAL or ORNL fission models) and ABLA for de-excitation [3].

1.4.1 *Stages of physical process in projectile interaction with a nucleus.* The brief overview of the processes is given as follows:

The intranuclear cascade model (INC) first proposed by Serber in 1947 [6] says that in particle–nuclear collisions, the de Broglie wavelength of the incident particle is comparable to or shorter than the average intranuclear distance.

In inelastic particle–nucleus collisions, fast phase (10^{-23}–10^{-22} s) of INC results in a highly excited nucleus, and is followed by fission and pre-equilibrium emission. A slower (10^{-18}–10^{-16} s) compound nucleus phase follows with evaporation. Pre-equilibrium model was introduced by Gudima *et al* [7] and Prael *et al* [8] as another model between INC and de-excitation.

Multistep pre-equilibrium exciton model (MPM) is used after INC step; in fact the MPM model is invoked after completion of INC, with the initial particle–hole configuration and excitation energy determined by the outcomes of the cascade. In any stage of MPM, the excited nucleus may emit a neutron, proton, deuteron, triton, alpha and ^{3}He alternatively. The MPM terminated upon reaching the equilibrium exciton number and the evaporation model is applied to release its remaining energy by the excited nucleus [9].

The necessary condition for the INC model to be valid is $\lambda B/v \ll \tau c \ll \Delta t$, where λB is the de Broglie wavelength of the nucleons, v is the average relative nucleon–nucleon velocity and Δt is the time interval between collisions. The physical foundation becomes approximate at energies less than about 200 MeV, and a pre-equilibrium model is needed as a supplement [10].

1.4.2 *BERTINI model.* The common feature of the BERTINI model is the approximation of the real nuclear density distribution by concentric zones having constant density. BERTINI model presents three-zone division for a nucleus.

In BERTINI model, the nucleus is modelled as a continuous medium in which the incident particles collide with a nucleon according to its mean free path. This nucleon then can be set into motion and can undergo further collisions. The stopping criterion of the model is the cut-off energy. Cascade propagation occurs by the collided particles

which are transported based on BERTINI model. In the model the 'strict' Pauli principle is used to control the application of the Pauli principle [9–11].

1.4.3 *ISABEL model.* The ISABEL model implies the division of the nucleus in sixteen zones. The main difference between all the models is the approaches used for the intranuclear (INC) interaction simulation, determination of the point of particle interaction, selection of collision partners for the moving nucleons and pions and the parametrization of n–n and p–n cross-sections. In ISABEL, the nucleus is modelled as a continuous medium in which the incident particles collide according to its mean free path with a nucleon as well. This nucleon is then set into motion and can undergo further collisions. The stopping criterion of the model is the cut-off energy.

When ISABEL INC is invoked, it is possible to determine explicitly the particle–hole of residual nuclei since a count of the valid excitations from the Fermi sea is provided. The nucleons follow linear trajectories between collisions, the target Fermi motion is taken into account, free nucleon–nucleon cross-sections are used, inelastic nucleon–nucleon collisions involving excitation of delta resonance and creation of pions are included and the Pauli blocking inhibits collisions leading to the already occupied states [9–11].

1.4.4 *CEM03 model.* CEM03 model is another accessibility model inserted in MCNX 2.6. The coalescence, pre-equilibrium, evaporation, fission and Fermi break-up models used by the last versions of the cascade-exciton model event generator CEM03.03 have been extended recently to improve the description of complex particle production from nuclear reactions. The CEM03.03 code calculates nuclear reactions induced by nucleons, pions and photons. It assumes that reactions occur generally in three stages: the intranuclear cascade (INC) stage, the pre-equilibrium stage and the equilibrium evaporation/fission stage. CEM03.03 uses the coalescence model to 'create' high-energy d, t, ^{3}He and ^{4}He by final-state interactions among emitted cascade nucleons. However, if the residual nuclei after INC have mass numbers with $A < 12$, CEM03 uses the Fermi break-up model to calculate their further disintegration instead of using the pre-equilibrium and evaporation models [12,13].

1.4.5 *INCL4 model.* INC models describe interactions between an impinging particle and target nucleons during intranuclear cascade as a sequence of binary collisions separated in space and time. This is valid if the wavelength of the incident particle is smaller than the mean distance between nucleons of the target nucleus; the mean free path of the incident particle in the target nucleus is greater than the internucleon lengths. The trajectory between collisions is assumed to be linear. The collisions proceed until a certain degree of equilibrium is reached.

The criterion used in the INC model of Cugnon (INCL4) is the empirical time of equilibrium (the so-called cut-off time $t_{\text{cut}} \approx 30$ fm/c that allows five sequential nucleon–nucleon interactions on the average), which is deduced from a clear change of the calculated quantities (like the integral number of emitted particles, their total kinetic energy or the excitation energy of the residual nucleus). In INCL4, the Saxon–Woods density distribution is used and cut at the radius is described with a diffuseness parameter.

Fermi motion of the nucleons and the quantum effects of Pauli blocking are taken into account [14–17].

2. Material and methods

Cross-sections of ^{109}Cd, ^{85}Sr and ^{86}Y due to 15 MeV protons induced on ^{nat}Ag, ^{nat}RbCl and $^{nat}SrCO_3$ targets were calculated by ALICE ASH 1.0 and TALYS 1.0 codes.

15 MeV proton range and the target stopping power were calculated for all the mentioned targets using SRIM code. A theoretical production yield was calculated using ALICE ASH 1.0, TALYS 1.0 and SRIM data by integrating over the achieved discrete cross-sections using Simpson numerical method.

The target irradiation conditions such as the beam profile, target and its substrate were modelled in MCNPX 2.6 code. The thickness of the target material was calculated using SRIM code according to 0 up 15 MeV energy range. The target material deposited on copper substrate was modelled in identical dimensions with the experimental used by cyclotron accelerators. Five water grids of 2 mm thickness have been loaded in the lower surface of the copper substrate. Proton beam of identical FWHM with CYCLON30 has been introduced in SDEF card. The target system was placed in 6° angle (figure 1). HISTP card was used to report a proton source in target cell during nuclear reaction calculations. HTAPE3X.exe was used to calculate the amount of impurities using IOPT CARD; the particle transport history of 10000000 was selected to reduce calculation errors to less than 0.1%. Different INC physical models of BERTINI/DENSER, BERTINI/ABLA, INCL4/DENSER, INCL4/ABLA, ISEBEL/DENSER, ISABEL/ABLA and CEM were used to calculate production yields to determine the best physical model. The residuals' activity in the target was compared with the ALICE ASH 1.0 and TALYS 1.0 data as well as the experimental. Relative discrepancy between theoretical and experimental was determined as follows:

$$\text{Relative discrepancy} = \left(\frac{\text{Exp.} - \text{Cal.}}{\text{Exp.}} \times 100\right) \quad (\%)\,. \tag{2}$$

Water grids were modelled approximately similar to their real shape because they have no noticeable influence on the production yield.

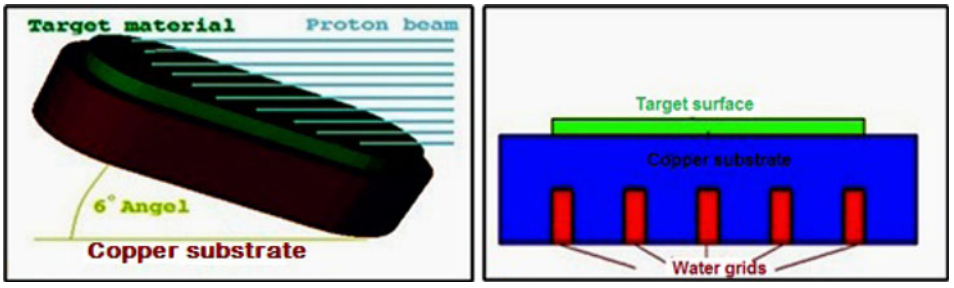

Figure 1. (**a**) Schematic of the modelled target in MCNPX 2.6, (**b**) longitudinal view.

2.1 *Experimental procedure for the production of radioisotopes*

Irradiation of the targets was carried out at the AMIRS (Agricultural, Medical and Industrial Research School) employs a Cyclone-30 (IBA, Belgium).

2.1.1 ^{85}*Sr production.* To produce ^{85}Sr radioisotope, target layers of fine powdered RbCl were prepared by the sedimentation technique by which the powder was deposited on the elliptical copper substrate (11.69 cm^2 surface area) [18]. The coated natural RbCl was introduced into a target holder and bombarded with 15 MeV protons at a current of 5 mA for 5 min. Irradiated rubidium chloride was removed from substrate using 50 ml of water-free acetone. The radioactivity of the sample solution was determined using high-resolution HPGe detectors. The distance of the sample from the detector was 30 cm. The counting time was adjusted according to the half-life of the product nuclide to get reasonable counting statistics. All the major γ-lines of the resulting radionuclides were identified. The ^{85}Sr activity was determined using 514 keV γ-rays. Yields of about 1.4 MBq/μAh were experimentally obtained. The experimental yield and the experimental data of Qaim *et al* agree with each other at least within 6% relative discrepancy [19,20].

2.1.2 ^{109}*Cd production.* Electrodeposition of silver on copper substrate was carried out using alkaline plating bath for producing ^{109}Cd through the ^{nat}Ag(p, n)^{109}Cd nuclear reaction. The alkaline plating bath of optimum compositions of 4.1 g/1 silver, pH 10–12, DC current density of 4.27 mA·cm^{-2} at 40–50°C temperature resulted in 100% current efficiency for 59 μm silver deposition on copper substrate. The target was irradiated by 15 MeV proton beam current of 150 μA for 10 min. The target material was dissolved efficiently by a liquid flow-through stripper acidic system (40 ml, 14 M HNO_3 at room temperature). The analysis of the solution using high-resolution HPGe detector showed a 1.88 μCi/μAh (0.069 MBq/μAh) ^{109}Cd production, but it was less than Landin *et al's* experimental data with about 3% relative discrepancy [21,22].

2.1.3 ^{86}*Y production.* The deposition of strontium carbonate on copper substrate was carried out by the sedimentation method in order to produce ^{86}Y. Thick layer of natural strontium carbonate was prepared with 480 mg $SrCO_3$, 220 mg ethyl cellulose and 7.5 ml acetone. The deposited target was irradiated at 30 μA current and 15 MeV proton beam for 12 min. After bombardment of the deposited $^{nat}SrCO_3$, 2201 μCi of ^{86}Y was obtained [23–25].

3. Result and discussion

According to the SRIM output plotted in figure 2, minimum dimension needed for rubidium chloride, strontium carbonate and silver targets was determined (table 1).

However 2490, 2060 and 485.93 μm thickness are needed in 0→15 MeV proton range for RbCl, $SrCO_3$ and Ag targets respectively according to SRIM output plotted in figure 2,

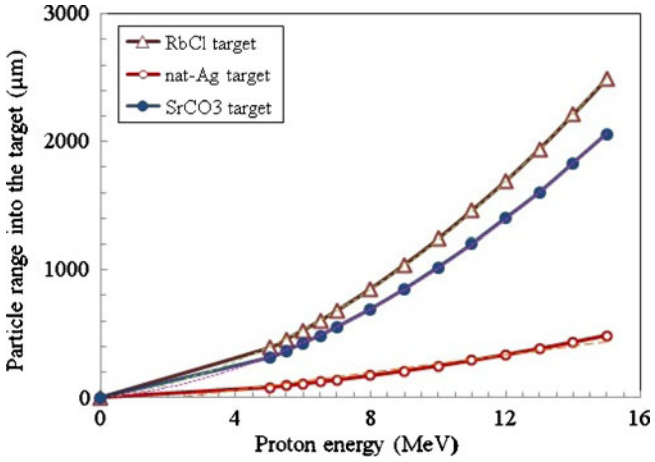

Figure 2. Calculation of proton range in the targets using the SRIM code.

the target thicknesses being chosen similar to the experimental ones in all simulations (table 1).

The cross-sections of the targets due to their proton-induced reactions were achieved by ALICE ASH 1.0 and TALYS 1.0 codes (figures 3 and 4). As can be clearly seen in figure 3, increasing the proton energy more than 15 MeV does not increase the production yields considerably. As can be seen, the obtained cross-sections via the deterministic codes are in good confirmation with each other.

The theoretical reaction yields were calculated using the achieved cross-sections and stopping power values. The results show that there is about 14.05–221.67% relative discrepancies between the deterministic code and experimental data (tables 2 and 3). The theoretical calculated yields are closer to experimental yields using ALICE ASH 1.0 code.

The currents used in experimental irradiations mentioned in table 1 were used to transform IOPT card output (per source particle) to all particle sources.

The beam profile was shown in figure 5 using MESH-tally card of MCNPX 2.6. As can be seen, a similar irradiation circumstance with experimental cyclotron target irradiation was used in the simulation.

Table 1. The targets and irradiation characteristics [19,21,23].

Target	Thickness (μm)	Thickness/6° beam geometry SRIM 5 → 15 MeV (μm)	Thickness/6° beam geometry Exp. 5 → 15 MeV (μm)	Current (μA)	Irradiation time (min)
$SrCO_3$	1750	175	131.69	30	12
RbCl	2100	210	172.5	5	5
Ag	590	40.5	59[a]	150	10

[a]Additional thickness was provided to reduce the copper impurity in the solution of irradiated target.

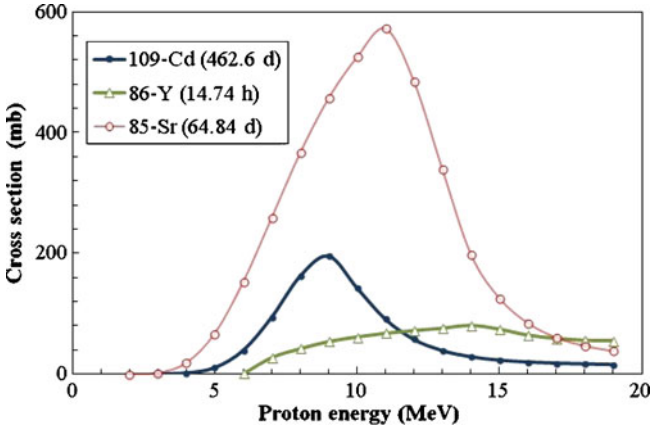

Figure 3. Calculation of proton-induced cross-sections on the natural targets using ALICE ASH 1.0.

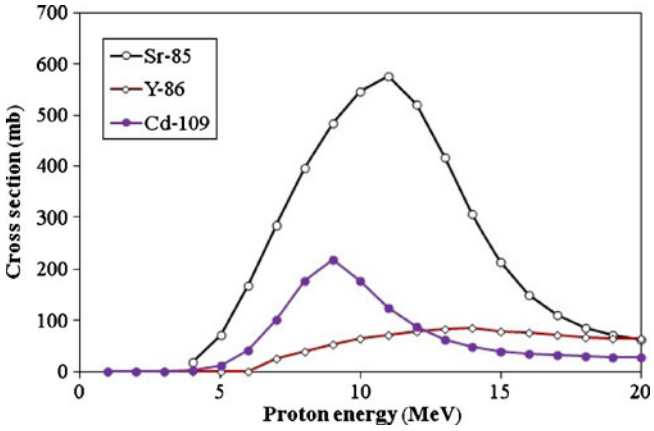

Figure 4. Calculation of proton-induced cross-sections on the targets using TALYS 1.0.

Table 2. Comparison of ALICE ASH 1.0 and experimental data [19,21,23].

Radioisotope	ALICE ASH (μCi)	Exp. (μCi)	Relative discrepancy (%)	Comment
^{109}Cd	53.15	46.60	14.05	Overestimated
^{85}Sr	29.48	15.76	87.05	Overestimated
^{86}Y	6660	2201	202.58	Overestimated

The theoretical yields of the radioisotope were calculated using the IOPT and the stochastic codes. The results showed that ISABEL/ABLA, BERTINI/DENSER and ISABEL/DENSER obtain the least discrepancies with the experimental data (table 4).

Table 3. Comparison of TALYS 1.0 and experimental data [19,21,23].

Radioisotope	TALYS (μCi)	Exp. (μCi)	Relative discrepancy (%)	Comment
^{109}Cd	68.75	46.60	47.53	Overestimated
^{85}Sr	33.81	15.76	145.53	Overestimated
^{86}Y	7080	2201	221.67	Overestimated

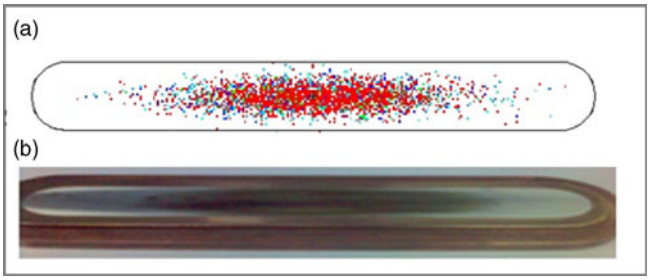

Figure 5. View of the proton beam profile used on the targets using MCNPX 2.6. (**a**) Surface view of the target and (**b**) real irradiated target.

Table 4. Comparison of physical models of MCNPX 2.6 to produce the isotopes using 15 MeV proton.

Isotope	BERTINI/ DENSER (μCi)	INCL4/ DENSER (μCi)	CEM (μCi)	BERTINI/ ABLA (μCi)	INCL4/ ABLA (μCi)	ISABEL/ ABLA (μCi)	ISABEL/ DENSER (μCi)	Exp. (μCi)
^{109}Cd	110.25	109.2	142.18	220.61	359.24	101.34	125.89	46.60
^{85}Sr	20.12	29.38	34.98	17.70	29.20	17.39	20.26	15.76
^{86}Y	4024.54	3833.88	4249.32	4832.82	4473.90	4832.82	3712.38	2201

Result showed using ISABEL/ABLA physical model in all MCNPX 2.6 simulations concluded that the closest data to the experimental yields have average relative discrepancies of about 82% (table 5). Computational stochastic MCNPX 2.6 code can estimate the production yields in more conformity with experimental data than the ALICE ASH 1.0 and TALYS 1.0 deterministic codes.

Calculation of ^{85}Sr yield in different energies of the projectile using the computational method showed that all the physical models studied are in a good conformity with each other up to 11 MeV. But the evaluated cross-sections showed that the production yield will not have noticeable enhancement between 11 and 15 MeV which means the yield curve should reveal an approximately smooth behaviour through this range, and INCL4/ABLA, INCL4/DENSER and CEM03 models are not efficient to estimate the yield in this energy range (figure 6).

Table 5. Comparison of MCNPX 2.6 and experimental data.

Radioisotope	ISABEL/ABLA (μCi)	Exp. (μCi)	Relative discrepancy (%)	Comment
^{109}Cd	101.34	46.60	117.46	Overestimated
^{85}Sr	17.39	15.76	10.40	Overestimated
^{86}Y	4832.82	2200	119.57	Overestimated

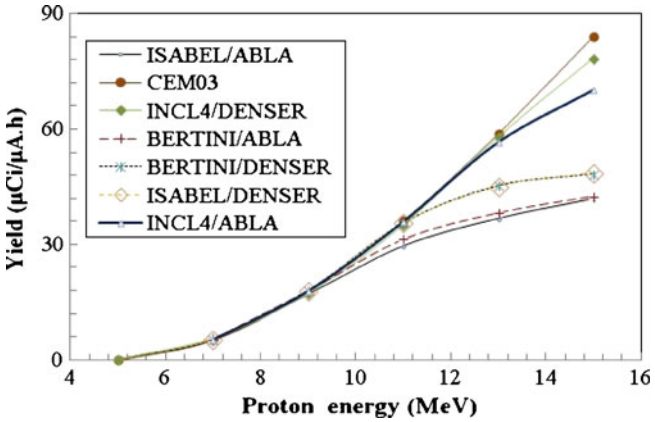

Figure 6. Comparison of different physical models to produce ^{85}Sr via ^{nat}Rb (p, n)^{85}Sr reaction.

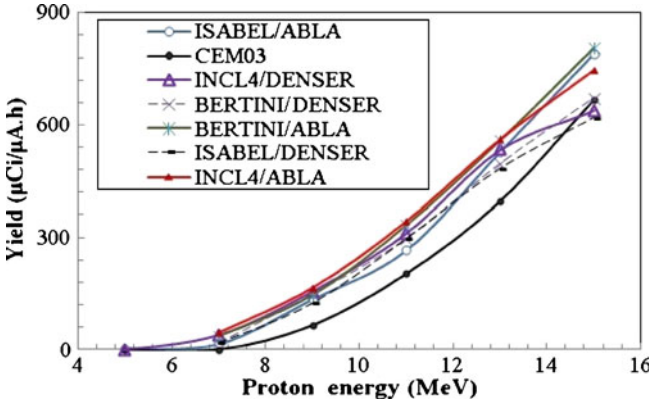

Figure 7. Comparison of different physical models to produce ^{86}Y via ^{nat}Sr(p, n)^{86}Y reaction.

In the case of ^{86}Y, yield plots on projectile energy indicate that all the studied physical models are approximately in conformance with each other up to 13 MeV except CEM03. Discrepancies between the models increase between 13 and 15 MeV (figure 7).

Using different physical models to calculate ^{109}Cd yield indicate high discrepancies between the models especially for BERTINI/ABLA and INCL4/ABLA models which

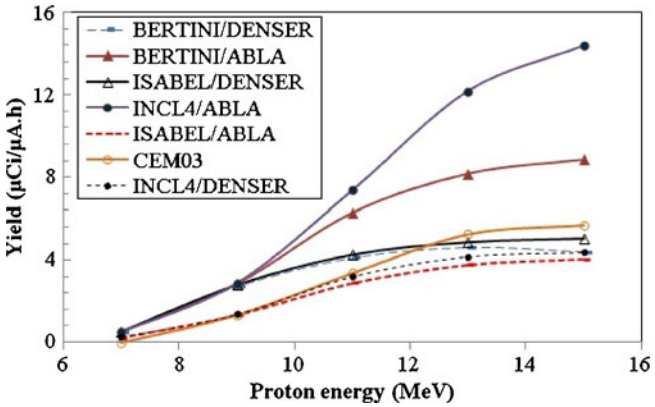

Figure 8. Comparison of different physical models to produce ^{109}Cd via ^{nat}Ag(p, n)^{109}Cd reaction.

are far from the others in all the energy ranges. It seems BERTINI/DENSER and ISABEL/DENSER models are sufficient to estimate the production yield (figure 8).

Comparison between the deterministic code data and MCNPX 2.6 showed that ^{85}Sr yield using INCL4/DENSER and ISABEL/DENSER models are in good agreement with ALICE ASH 1.0 and TALYS 1.0 data in all energy ranges (figure 9).

Comparison between the deterministic code data and MCNPX 2.6 showed that ^{86}Y yield using ISABEL/DENSER model is in good agreement with ALICE ASH 1.0 and TALYS 1.0 data up to 11 MeV (figure 10). It can be said that this model is the best one compared to others according to the prior evaluations.

Comparison between the deterministic code data and MCNPX 2.6 showed that ISABEL/ABLA model yield has the most conformances than the others to estimate ^{109}Cd

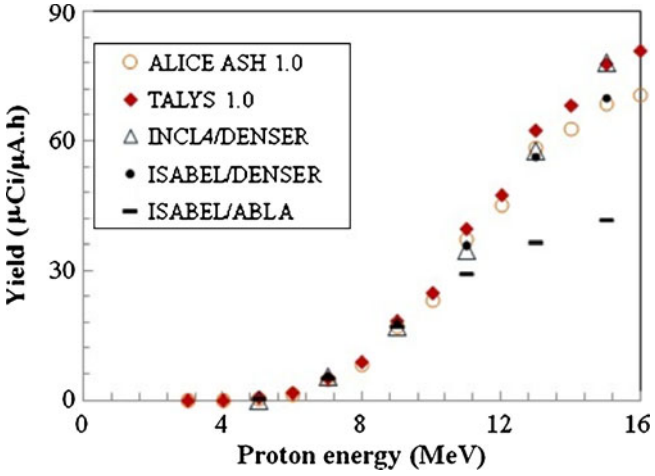

Figure 9. Comparison of different ALICE ASH 1.0 and TALYS 1.0 codes to produce ^{85}Sr via ^{nat}Rb(p, n)^{85}Sr reaction.

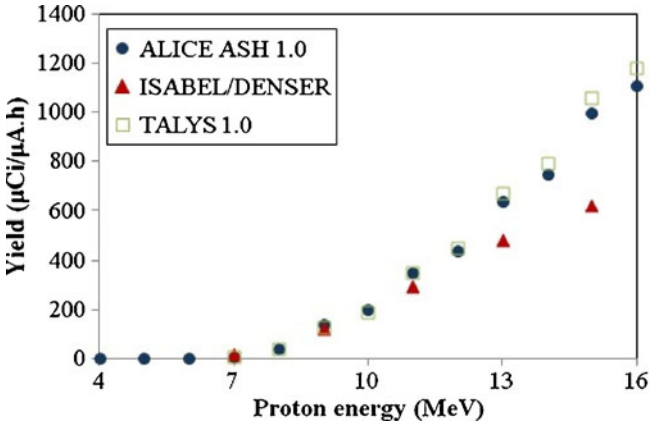

Figure 10. Comparison of different ALICE ASH 1.0 and TALYS 1.0 codes to produce ^{86}Y via ^{nat}Sr(p, n)^{86}Y reaction.

production while the model has noticeable discrepancies with the deterministic codes' data, ALICE ASH 1.0 and TALYS 1.0 (figure 11). The ISABEL/ABLA model can be suggested as the most efficient model for calculating the radioisotope yield.

3.1 *Validation of INC for low-energy projectiles*

However, the INC is traditionally applied to reactions above 100 MeV nucleon energy, in which N–N (nucleon-nucleon) collisions play a prominent role. The most important

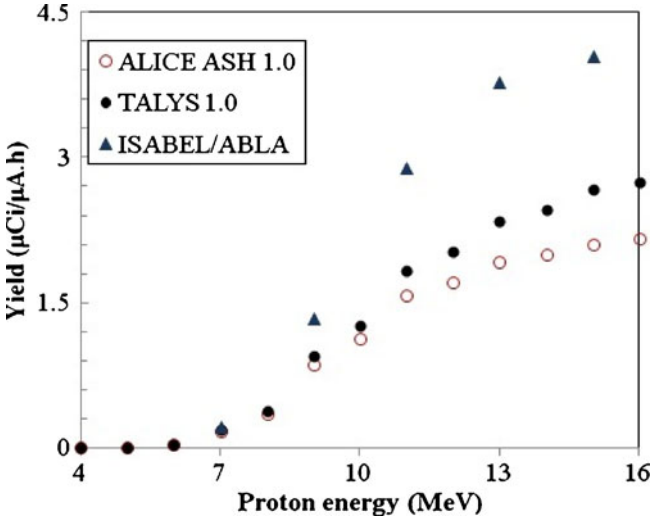

Figure 11. Comparison of different ALICE ASH 1.0 and TALYS 1.0 codes to produce ^{109}Cd via ^{nat}Ag(p, n)^{109}Cd reaction.

feature in the propagation of a low-energy nucleon in the nucleus is the medium effect on the free N–N interaction whose most essential features are the Pauli effect and the Fermi motion. Both the Pauli effect and the Fermi motion are already included in most of the INC calculations. Overall, the formulated INC calculation according to the results of Kim *et al* reproduces the total reaction cross-section very well over a wide range of target masses and beam energies, confirming the applicability of the INC for nucleon propagation in a nucleus, even at nucleon energies below 100 MeV. Hence, an INC can be applied reasonably well to study the systematics of the propagation of nucleons at low energies of a few tens of MeV [26].

Cugnon and Henrotte [27] reported a pragmatic approach, which compares the predictions of the Liège intranuclear cascade model with available data at incident energy between 40 and 250 MeV. Cugnon and Henrotte reported that this model gives surprisingly good results at energies well below the limit mentioned above [27].

Bertini *et al* [28] used one version of INC model and reported that this model showed unexpectedly good results for the nonelastic cross-section, when compared to data from lower energy (30–60 MeV) proton-induced reactions.

Overall, there is a necessity for complementary studies in INC model utilization for low-energy projectiles induced on different target materials to evaluate its validity in comparison with experimental data in this low-energy range.

However, the application of intranuclear cascade model for low-energy projectile concluded in good conformity with experimental in this work, but it cannot be used for all target elements and additional simulations are mandatory to evaluate the degree of INC model fitness for the other target elements bombarded with low-energy projectiles.

4. Conclusion

Accelerator-based radioisotopes have important applications in radiotherapy and radioimaging in medical science as well as in radiotracing in industry. Therefore, it is necessary to find an economical nuclear reaction which achieves lowest impurities along with highest radioisotope yield.

Nuclear codes such as ALICE ASH 1.0 and TALYS 1.0 which can efficiently calculate reaction cross-sections theoretically were used to evaluate the production yields. Over the deterministic codes, MCNPX 2.6 can model a reaction in stochastic method using experimental libraries.

Comparison of the calculated yields (using the ALICE ASH 1.0 and MCNPX 2.6) and experimental yields showed that MCNPX 2.6 have a reveal surpass for such calculations because average relative discrepancy of MCNPX 2.6 and experimental yields is 82% using the stochastic code and ISABEL/ABLA physical model. The average relative discrepancy value between ALICE ASH 1.0 and experimental will be 101%.

ALICE ASH 1.0 has considerable surpass compared to TALYS 1.0 code for such calculations because of more valid data in comparison with the experimental as can be obviously seen from the obtained data.

Hence, MCNPX 2.6 code is suggested as a powerful tool for more precise computing of a nuclear reaction and yield estimation of a radioisotope before its production.

Application of INC model for other target elements irradiated with low-energy projectiles should be studied as more complementary section of such benchmark studies.

References

[1] C H M Broeders, A Yu Konobeyev, A Yu Korovin, V P Lunev and M Blann, http://bibliothek.fzk.de/zb/berichte/FZKA7183.pdf (2006)
[2] J Koning, S Hilarie and M A Duijvestijn, NRC – Nuclear Research and Consultancy Group (2007)
[3] D B Pelowitz, LANL, LA-CP-07-1473 (2008)
[4] D I Poston and H R Trellue, PSR-455 RSICC, ORNL (2003)
[5] J F Ziegler, M D Ziegler and J P Biersack, SRIM manual part A (IBM Research, New York, USA, 2006)
[6] R Serber, *Phys. Rev.* **72**, 1114 (1947)
[7] K K Gudima, G A Ososkov and V D Toneev, *Sov. J. Nucl. Phys.* **21**, 138 (1975)
[8] R E Prael and M Bozoian, *Adaptation of the multistage preequilibrium model for the Monte Carlo method*, LA-UR-88-3238 (Los Alamos National Laboratory, USA, 1988)
[9] R P Prael, Los Alamos National Laboratory, USA, 145 (1989)
[10] C H M Broeders and A Yu Konobeyev, *Nucl Instrum. Methods in Phys. Res. B* **234**, 387 (2005)
[11] S Leray, Nuclear reaction at high energy, *Workshop on Nuclear Data for Science and Technology* (2001)
[12] S G Mashnik, K K Gudima, A J Sierk, M I Baznat and N V Mokhov, Los Alamos, http://www-rsicc.ornl.gov/codes/psr/psr5/psr-532.html (2005)
[13] S G Mashnik, A J Sierk, K K Gudima and M I Baznat, *J Phys: Conf. Ser.* **41**, 340 (2006)
[14] H W Bertini, *Phys. Rev*. **131**, 1801 (1963)
[15] Y Yariv and Z Fraenkel, *Phys. Rev. C* **24**, 488 (1981)
[16] A Boudard, J Cugnon, S Leray and C Volant, *Phys. Rev. C* **66**, 044615 (2002)
[17] L Pienkowski, H G Bohlen, J Cugnon, H Fuchs, J Galin, B Gatty, B Gebauer, D Guerreau, D Hilscher, D Jacquet, U Jahnke, M Josset, X Ledoux, S Leray, B Lott, M Morjean, A Péghaire, G Röschert, H Rossner, R H Siemssen and C Stephan, *Phys. Lett. B* **336**, 147 (1994)
[18] M Sadeghi, Z Alipoor and T Kakavand, *NUKLEONIKA* **55**, 303 (2010)
[19] S M Qaim, G F Steyn, I Spahn, S Spellerberg, T N Walt and H H Coenen, *Appl. Radiat. Isot*. **65**, 247 (2007)
[20] M Sadeghi, Z Alipoor and G Aslani, *KERNTECHNIK* **76**, 373 (2011)
[21] M Sadeghi, M Mirzaee, Z Gholamzadeh, A Karimian and F Bolourinovin, *Radiochim. Acta* **97**, 113 (2009)
[22] M Mirzaee, M Sadeghi, Z Gholamzadeh and Shapour Lahouti, *J. Radioanal. Nucl. Chem*. **277**, 645 (2008)
[23] M Sadeghi, A Zali and G Aslani, *KERNTEKNIK* **76**, 373 (2011)
[24] M Sadeghi, A Zali, M Aboudzadeh, P Sarabadani, G Aslani and A Majdabadi, *Appl. Radiat. Isot*. **67**, 2029 (2008)
[25] M Sadeghi, M Aboudzadeh, A Zali and B Zeinali, *Appl. Radiat. Isot*. **67**, 1392 (2009)
[26] M J Kim, H Bhang, J H Kim, Y D Kim, H Park and J Chang, *J. Kor. Phys. Soc*. **46(4)**, 805 (2005)
[27] J Cugnon and P Henrotte, *Eur. Phys. J. A* **16**, 393 (2003)
[28] H W Bertini, G D Harp and F E Bertrand, *Comparisons of predictions from two intranuclear-cascade models with measured secondary proton spectra at several angles from 62- and 39-MeV protons on various elements*, U.S. Atomic Energy Commission Report